not understand why this early apatite mineralization seemingly affected so few embryos, despite the multitudes probably laid, and did not lead to any soft tissue preservation for other fossils even though there was widespread phosphatization of calcitic skeletons in the Duyun fauna. These embryos preserve no obvious microbes, so we cannot ascertain whether bacterial activity was involved in the phosphatization process, as has been suggested (*6*, *18*, *19*).

REFERENCES AND NOTES

1. S. G. Katz and J. Sprinkle, *Science* **192**, 1137 (1976).
2. J. Barrande, *Systême Silurien du Centre de la Bohême Ière Partie: Recherches Paléontologiques*, vol. 1 of *Crustacés, Trilobites* (self-published, Prague and Paris, 1852); C. E. Beecher, *Am. Geol.* **16**, 166 (1895).
3. S. E. Speyer and B. D. E. Chatterton, *Hist. Biol.* **3**, 27 (1989).
4. X.-G. Zhang, *Alcheringa* **11**, 1 (1987).
5. R. H. Bate, *Palaeontology* **15**, 379 (1972).
6. D. E. G. Briggs, A. J. Kear, D. M. Martill, P. R. Wilby, *J. Geol. Soc. London* **150**, 1035 (1993).
7. Cambrian spheres *Archaeooides* and *Olivooides* found from several localities in China were all described as fossils of uncertain systematic position because of their simple, nondiagnostic morphology. Some of them are oval-shaped [X. Yang, Y. He, S. Deng, *Bull. Chengdu Inst. Geol. Mineral. Resour. Chinese Acad. Geol. Sci.* **4**, 91 (1983); P. Chen, *Prof. Pap. Strat. Palaeontol.* **13**, 49 (1984)] and may be eggshells, but published illustrations are insufficient to demonstrate this.
8. M. da S. P. Regali and W. A. S. Sarjeant, *Micropaleontology* **32**, 163 (1986).
9. L. F. Gall and B. H. Tiffney, *Science* **219**, 507 (1983).
10. Egg size and morphology may vary within genera and species of some living crustaceans [G. Mura, *Crustaceana* **61**, 241 (1991); *ibid.* **63**, 225 (1992)] and chelicerates (*14*).
11. The thickness of the shell is measurable in three of the eggs under a SEM. An outermost layer, 0.5 μm thick, is determined in three eggs (Fig. 1, A, B, C, and E).
12. Dimples on part of the surface of the fifth embryo resemble those on the blastomeres of extant crayfish embryos [J. D. Celada, P. de Paz, V. R. Gaudioso, R. Fernández, *Anat. Rec.* **219**, 304 (1987); J. D. Celada, J. M. Carral, J. González, *Crustaceana* **61**, 225 (1991)] and may reflect partial collapse of these cells.
13. During the embryonic process, the surface area of an embryo can be considered as a constant even though the number of blastomeres increases with growth. Considering, in the simplest case, polygons on the outer surface of a shell to be all hexagons, the surface area (*A*) of the embryo is

$$A = \frac{3\sqrt{3}}{2}(s_1^2 + s_2^2 + \ldots + s_n^2) \approx \frac{3\sqrt{3}}{2} nS^2$$

where *s* is the length of a side of a hexagon, *S* is the average length of all measured sides, and *n* is the total number of hexagons. Therefore, for any two embryos, their equal surface areas can roughly be expressed as

$$\frac{3\sqrt{3}}{2} n_1 S_1^2 = \frac{3\sqrt{3}}{2} n_2 S_2^2$$

or $n_1/n_2 = S_2^2/S_1^2$. If the number of blastomeres would double in the subsequent division stage (that is, $n_1/n_2 = 2$) then $S_1/S_2 = \sqrt{2}/2$. The average length S_1 of the third embryo is about 0.008 mm, and S_2 for the first two embryos showing blastomeres is 0.011 mm; $S_1/S_2 \approx 0.7 \approx \sqrt{2}/2$.
14. K. Sekiguchi, Y. Yamamichi, H. Seshimo, H. Sugita, in *Biology of Horseshoe Crabs*, K. Sekiguchi, Ed. (Science House, Tokyo, 1988), pp. 133–224.
15. D. T. Anderson, in *Arthropod Phylogeny*, A. P. Gupta, Ed. (Van Nostrand Reinhold, New York, 1979), pp. 59–105; R. Nagabhushanam and R. Sarojini, *Invertebrate Embryology* (Oxford, New Delhi, 1985).
16. Trilobita are closely related to Crustacea and Chelicerata [D. E. G. Briggs and R. A. Fortey, *Science* **246**, 241 (1989); G. Budd, *Nature* **364**, 709 (1993)]. The four fossil embryos exhibiting blastomeres are much smaller than, but otherwise appear comparable to, stage 2 and stage 3 embryos of modern horseshoe crabs (*14*), and their shells are similarly laminated.
17. Of the associated youngest trilobite instars, the protaspis of the unidentified polymeroid trilobite is about 0.50 mm long and wide, whereas the protaspis of *Pagetia* sp. is about 0.25 mm in our collection and 0.28 to 0.35 mm in previously reported specimens [J. H. Shergold, *Alcheringa* **15**, 65 (1991)]. On the basis of size, the five embryos are more likely those of an eodiscid trilobite.
18. D. M. Martill, *Nature* **346**, 171 (1990); D. E. G. Briggs and A. J. Kear, *Science* **259**, 1439 (1993).
19. D. M. Martill, *Palaeontology* **31**, 1 (1988); P. A. Allison, *Paleobiology* **14**, 331 (1988).

20. This work was supported by the Natural Sciences and Engineering Research Council of Canada. We thank D. M. Lehmkuhl and D. M. Martill for criticizing an earlier version of the manuscript and Y. Yano for assistance with SEM photography.

7 June 1994; accepted 30 August 1994

Role of Oocyte Position in Establishment of Anterior-Posterior Polarity in *Drosophila*

Acaimo González-Reyes and Daniel St Johnston*

The polarized microtubule cytoskeleton of the *Drosophila* oocyte directs the localization of the maternal determinants which establish the anterior-posterior (AP) axis of the embryo. Because the formation of this microtubule array is dependent on signals from the follicle cells that surround the oocyte, it has been proposed that AP polarity originates in the follicle cells. Here it is shown that the movement of the oocyte to the posterior of the egg chamber early in oogenesis determines AP polarity in the follicle cell layer, and also in the oocyte. Moreover, the generation of AP asymmetry requires signaling from the germ line to the soma and back again.

The AP axis of the *Drosophila* embryo is defined during oogenesis by the localization of the maternal determinants bicoid and oskar mRNAs to opposite poles of the oocyte (*1–4*). When these transcripts first localize, the oocyte cytoskeleton shows clear AP asymmetry: The microtubule-nucleating activity lies at the anterior of the cell, and the plus ends of the microtubules extend toward the posterior pole (*5*, *6*). Because the transport and anchoring of bicoid and oskar mRNAs is microtubule dependent (*6*, *7*), AP polarity within the oocyte is defined by the organization of the cytoskeleton. The formation of this polarized microtubule array depends, at least in part, on signals from the somatic follicle cells that surround the germline cyst (15 nurse cells and the oocyte), because the removal of *Notch* or *Delta* function in the follicle cells generates two anterior poles within the oocyte (*8*). This result led to the proposal that AP polarity originates in the follicle cells (*9*). Because the first visible asymmetry in egg chamber development is the movement of the oocyte to the posterior of the germline cyst (Fig. 1A), an alternative possibility is that AP polarity arises with this movement. To investigate whether the placement of the oocyte at the posterior plays a role in axis formation, we examined the consequences of changes in oocyte position on the determination of follicle cell fates and on the development of AP polarity. To do this, we took advantage of mutations at the *spindle*-C locus (*spn-C*)(*10*), a maternal effect gene that is required for the correct positioning of the oocyte early in oogenesis. In ~60% of *spindle-C*^{094} mutant egg chambers, the oocyte fails to move to the posterior and lies either at the anterior of the germline cyst or in the middle, with nurse cells on both sides (bipolar) (Fig. 1B) (*11*). This phenotype has also been described for *dicephalic* mutants (*12*).

In a wild-type egg chamber, follicle cell behavior shows several AP asymmetries (*13*). During stage 9 of oogenesis (*14*), most of the follicle cells migrate posteriorly over the nurse cells to form a columnar layer that surrounds the oocyte (Fig. 2A). Shortly thereafter, 6 to 10 follicle cells at the anterior tip of the egg chamber (the border cells) migrate between the nurse cells to reach the anterior of the oocyte. Once the columnar follicle cells have covered the exterior of the oocyte, the most anterior of these cells migrate centripetally to separate the oocyte from the nurse cells (Fig. 2C). Both the border cells and the centripetal follicle cells express a gene called *slow border cells* [*slbo* (*15*)] and eventually collaborate to produce the micropyle, an anterior structure of the egg shell (Fig. 2E). In bipo-

The Wellcome/CRC Institute and Department of Genetics, University of Cambridge, Cambridge CB2 1QR, England.

*To whom correspondence should be addressed.

lar egg chambers, the altered arrangement of the germline cells induces a duplication of all these anterior follicle cell behaviors: The cells that cover both sets of nurse cells migrate toward the middle to form a belt around the oocyte (Fig. 2B), whereas two sets of *slbo*–expressing border cells and centripetal follicle cells migrate to cover both ends of the oocyte (Fig. 2D). Furthermore, the *slbo*-positive cells at the posterior form a second micropyle (Fig. 2F) instead of the normal posterior aeropyle, which demonstrates that these follicle cells have adopted an anterior fate.

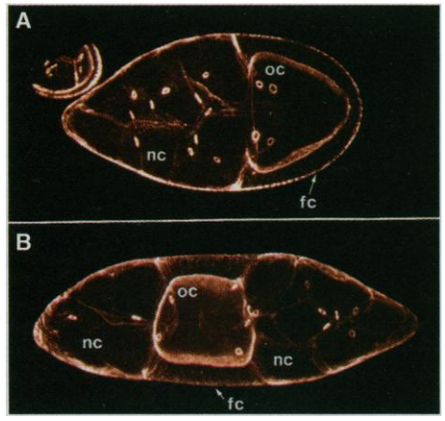

Fig. 1. F-actin staining (*26*) of wild-type and mutant egg chambers to visualize the shapes of the cells and the distribution of the ring canals. A wild-type egg chamber contains a cyst of 16 germline cells that are interconnected by F-actin–rich cytoplasmic bridges called ring canals. The oocyte, which possesses four ring canals, lies posterior to the 15 polyploid nurse cells. These germline cells are completely covered by a layer of somatic follicle cells from early in oogenesis onward. During the course of oogenesis, the follicle cells divide several times and most move backward to envelop the oocyte as it grows [reviewed in (*13*)]. (**A**) Wild-type egg chamber showing the columnar follicle cells (fc), the ring canals, the nurse cells (nc), and the oocyte (oc). (**B**) Bipolar egg chamber from a *spn-C*^{094} female. The normal arrangement of the 15 nurse cells and the oocyte is disrupted. Despite its abnormal, central position, a bipolar oocyte develops normally in several respects: it becomes surrounded by the follicle cells; it stores yolk and accumulates molecules specifically transported to the oocyte such as bicoid, oskar, K-10, and gurken mRNAs and Staufen protein (Fig. 3) (*3, 4, 18, 20, 21*); it possesses four ring canals; and its nucleus forms a karyosome (*14, 25*). Original magnification ×200.

Although these observations suggest that the oocyte must be at the posterior to induce posterior follicle cell fate, it is also possible that *spindle*-C activity is required in the follicle cells for their proper determination. To distinguish between these alternatives, we have generated mosaic egg chambers in which the germline cells are mutant for *spindle*-C, but the follicle cells are wild type (*16*). Germline clones have a strong bipolar phenotype identical to that seen when all cells of the egg chamber are mutant: The follicle cells migrate over both sets of nurse cells to form a layer around the oocyte, and a group of anterior follicle cells produces a micropyle at each pole of the oocyte (Fig. 2G, G' and G"). Thus, changes in follicle cell fate are a consequence of the misplacement of the oocyte, not the result of loss of *spindle*-C gene activity in the follicle cells themselves. These results indicate that the position of the oocyte at the posterior of the egg chamber is required for the acquisition of posterior follicle cell fate.

The position of the oocyte not only determines the fate of the follicle cells, it also directs their migration. The columnar follicle cells migrate to surround the oocyte wherever it lies in the egg chamber (Fig. 2B) (*17*). Furthermore, the border cells reach the oocyte even when it occupies only a small area on one side of the egg chamber (Fig. 2H). Such border cells migrate between fewer nurse cells with altered topology in order to reach their destination. These observations suggest that the oocyte produces specific signals that guide follicle cell movement.

The AP axis of the oocyte is also strongly affected in bipolar egg chambers. In bi-

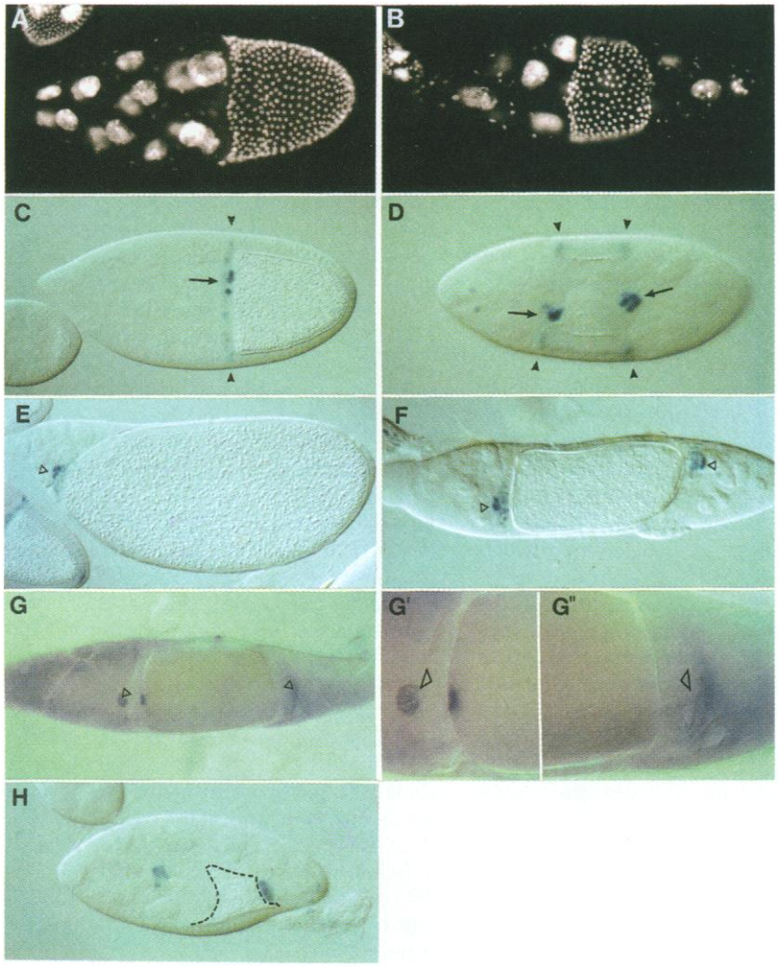

Fig. 2. Behavior of somatic follicle cells in wild-type and bipolar egg chambers. (**A** and **B**) Surface view of a wild-type and a mutant egg chamber stained with the DNA dye Hoechst (*27*). The large nuclei correspond to polyploid nurse cells and the small ones to follicle cells. In a normal egg chamber, as shown in (A), the posteriorly placed oocyte becomes surrounded by columnar follicle cells (*13*). In bipolar egg chambers, as shown in (B), the follicle cells over both sets of nurse cells migrate toward the center to form a belt around the oocyte. In (C to F and H) X-gal staining (*27*) shows *slbo* expression (*15*). (**C**) In wild-type egg chambers, the border cells undergo a migration from the tip of the egg chamber between the nurse cells to reach the anterior margin of the oocyte. The centripetal follicle cells migrate between the nurse cells and the oocyte. (**D**) In bipolar egg chambers, a second set of *slbo*-expressing border cells and centripetal follicle cells develop at the posterior. (**E**) Stage 13 wild-type egg chamber with the *slbo*-expressing cells around the developing anterior micropyle. (**F**) Bipolar egg chamber with *slbo*-expressing cells associated with a micropyle at each end. (**G**) Bipolar egg chamber from a germline clone. The oocyte and the nurse cells are mutant for *spn-C*. There are two sets of anterior follicle cells that produce micropyles (magnified in G' and G") at either end of the oocyte. (**H**) Bipolar egg chamber with a small oocyte. The border cells still migrate toward the oocyte, even when it only occupies a small lateral portion of the egg chamber. The dashed line displays the oocyte limits. Arrows, border cells; arrowheads, centripetal follicle cells; and open arrowheads, micropyles. Original magnification, ×200.

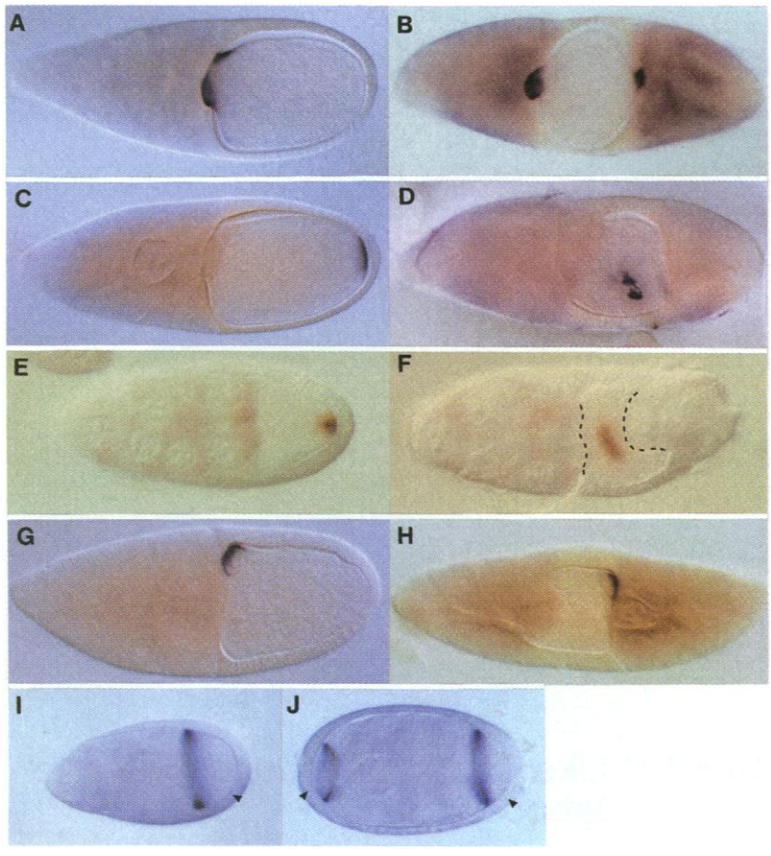

Fig. 3. Localization of bicoid, oskar, gurken, and K-10 mRNAs and kinesin–β-galactosidase protein in wild-type and mutant *spn-C* egg chambers (*28*). (**A**) The bicoid mRNA is localized to the anterior margin of the oocyte in wild-type egg chambers (*2, 3*). (**B**) In bipolar egg chambers, bicoid mRNA accumulates at the two poles of the oocyte which abut the nurse cells, as does another anteriorly localized transcript, K-10 mRNA (*20, 25*). (**C**) Normal localization of oskar mRNA to the posterior of the oocyte (*4*). (**D**) In mutant egg chambers, oskar mRNA localizes to the center of the oocyte. (**E**) Posterior accumulation of the kinesin–β-galactosidase protein (*6*) in a wild-type stage 9 egg chamber. (**F**) Central localization of the kinesin–β-galactosidase protein in a bipolar egg chamber. The oocyte-nurse cell borders are outlined. (**G**) The gurken mRNA normally accumulates on the dorsal-anterior margin of the oocyte nucleus (*21*). (**H**) In mutant egg chambers, gurken mRNA localization also depends on the position of the oocyte nucleus. Here, the nucleus is positioned adjacent to the posterior group of nurse cells. (**I**) Wild-type K-10 mRNA localization at the anterior pole of the oocyte (*20*). (**J**) A *spn-C* egg chamber with ~30 nurse cells and two oocytes, presumably due to an extra division during cyst formation. In each oocyte, K-10 mRNA is localized to the margin that faces the nurse cells. Arrowheads, oocytes. Original magnification, ×200.

polar oocytes, bicoid mRNA accumulates at both ends of the oocyte, rather than just at the anterior as in the wild type (Fig. 3, A and B), whereas Staufen protein (*18*) and oskar mRNA localize to the center of the oocyte, instead of to the posterior pole (Fig. 3, C and D). Because the localization of these products is microtubule dependent, one would expect that the microtubule network is altered in these *spindle*-C egg chambers. To test this, we used the plus end-directed motor kinesin attached to β-galactosidase as a marker for microtubule polarity (*19*). This chimeric protein accumulates at the plus ends of the microtubules at the posterior pole of a stage 9 wild-type oocyte (Fig. 3E) (*6*) and, like Staufen protein and oskar mRNA, localizes to the center of a bipolar oocyte (Fig. 3F). Thus, the altered arrangement of the nurse cells and oocyte causes a new mirror-symmetric organization of the microtubule cytoskeleton, which results in the transport of anterior components to each end of the oocyte and posterior pole plasm constituents to the plus ends of the microtubules in the center. Because both bicoid and oskar mRNAs localize normally in those follicles where the oocyte lies at the posterior, this mislocalization phenotype is a consequence of the misplacement of the oocyte and of the absence of posterior follicle cells and is not the result of the loss of *spindle*-C activity in the oocyte itself. Thus, AP polarity within the oocyte itself is defined by the position of the oocyte in the egg chamber. This is also true for egg chambers that possess two oocytes on either side of a single set of nurse cells. In such chambers, anteriorly localized transcripts, such as K-10 mRNA (*20*), accumulate in both oocytes at the margins that face the nurse cells (Fig. 3, I and J).

During mid-oogenesis, the oocyte nucleus moves to the future dorsal-anterior side of the cell in a microtubule-dependent process (*5*). In bipolar *spindle*-C or *dicephalic* egg chambers, the nucleus may lie at either end of the cell (*12*). Thus, the cellular machinery required for nucleus positioning can function at both ends of a bipolar oocyte, which supports the view that these

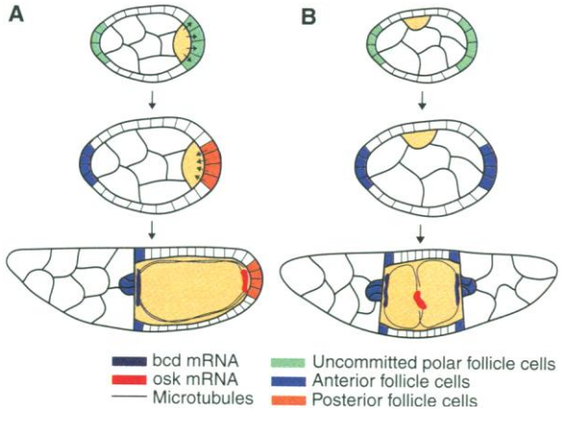

Fig. 4. A model for the origin of AP polarity in *Drosophila*. Three different stages of oogenesis are drawn (not to scale): before stage 7, stage 7–8, and stage 10a. (**A**) Wild type. The layer of follicle cells surrounding an early germline cyst contains a distinct group of cells at each pole, which can be distinguished by their expression of various enhancer trap lines (*13*). We propose that these polar follicle cells are initially uncommitted and are capable of adopting either an anterior or posterior fate. When the oocyte migrates to the posterior of the germline cyst, it comes into contact with the polar follicle cells at this end of the egg chamber and induces them to adopt a posterior fate. In the absence of this signal, the polar follicle cells at the opposite end of the egg chamber follow the default anterior pathway of development. During stage 7–8 (middle panel), the posterior follicle cells signal back to the oocyte to promote the disassembly of the microtubule-organizing centers at the posterior (*5*). Consequently, when the microtubule nucleating activity arises at the anterior end of the oocyte, it organizes a polarized microtubule network that extends to the posterior pole. This microtubule organization generates AP asymmetry by localizing bicoid and oskar mRNAs to opposite ends of the oocyte. (**B**) In bipolar egg chambers the misplacement of the oocyte prevents the induction of posterior follicle cell fate. As a consequence, both groups of polar follicle cells become anterior. The presence of two nurse cell–oocyte borders and the absence of posterior polar follicle cells leads to the formation of a symmetric microtubule cytoskeleton, resulting in the accumulation of bicoid mRNA at both sides of the cell and oskar mRNA in the center.

cells possess two anterior margins. The dorsal-ventral polarity of wild-type egg chambers is specified by the localization of gurken mRNA to the dorsal-anterior corner of the oocyte, adjacent to the nucleus (Fig. 3G) (*21*). In bipolar oocytes, gurken mRNA still accumulates above the nucleus, regardless of which end of the cell it lies (Fig. 3H). The localization of *gurken* transcripts therefore seems to be directed by the position of the oocyte nucleus and is not dependent on the duplicated microtubule cytoskeleton that localizes bicoid and oskar mRNAs.

On the basis of our observations, we propose that AP polarity in *Drosophila* originates with the movement of the oocyte to the posterior of the germline cyst, a process that requires the products of the *spindle-C*, *dicephalic*, and *armadillo* (*22*) genes, and at least three other loci on the third chromosome (*23*). This initial arrangement of the germline cells then determines all subsequent events in the establishment of anterior-posterior asymmetry in the egg chamber. To reconcile this model with the role of the follicle cells in the localization of maternal mRNAs in the oocyte, we suggest that the oocyte first induces posterior fate in the adjacent polar follicle cells, and that these follicle cells then signal back to the oocyte to reorganize the microtubule cytoskeleton, thereby defining AP polarity (Fig. 4). When this signaling fails, either as a result of the misplacement of the oocyte or a lack of somatic components required for the acquisition of follicle cell fate (*8*), the oocyte develops two anterior ends. Thus, like dorsoventral axis formation (*24*), the generation of anterior-posterior polarity involves signaling from the germ line to the somatic follicle cells, and from the follicle cells back to the germ line.

REFERENCES AND NOTES

1. D. St Johnston and C. Nüsslein-Volhard, *Cell* **68**, 201 (1992); A. Ephrussi and R. Lehmann, *Nature* **358**, 387 (1992).
2. T. Berleth *et al.*, *EMBO J.* **7**, 1749 (1988).
3. D. St Johnston, W. Driever, T. Berleth, S. Richstein, C. Nüsslein-Volhard, *Dev. Suppl.* **107**, 13 (1989).
4. J. Kim-Ha *et al.*, *Cell* **66**, 23 (1991); A. Ephrussi *et al.*, *ibid.*, p. 37.
5. W. E. Theurkauf, S. Smiley, M. L. Wong, B. M. Alberts, *Development* **115**, 923 (1992).
6. I. Clark *et al.*, *Curr. Biol.* **4**, 289 (1994).
7. N. J. Pokrywka and E. C. Stephenson, *Development* **113**, 55 (1991).
8. H. Ruohola *et al.*, *Cell* **66**, 433 (1991).
9. H. Ruohola-Baker, L. Jan, Y. Jan, *Trends Genet.* **10**, 89 (1994).
10. R. Tearle and C. Nüsslein-Volhard, *Drosophila Inf. Serv.* **66**, 209 (1987).
11. Other *spn-C* alleles, *spn-C*^{422} and *spn-C*^{660}, produce bipolar egg chambers with an identical phenotype to that produced by *spn-C*^{094}, although with a lower frequency (24 and 29%, respectively) (*25*). All the *spn-C* egg chambers shown are *spn-C*^{094}, except Fig. 3B which is *spn-C*^{422}.
12. M. Lohs-Schardin, *Wilhelm Roux's Arch. Dev. Biol.* **191**, 28 (1982).
13. A. Spradling, in *The Development of* Drosophila melanogaster, M. Bate and A. Martinez-Arias, Eds. (Cold Spring Harbor Laboratory Press, Cold Spring Harbor, New York, 1993), vol. 1, pp. 1–70.
14. A. Mahowald and M. Kambysellis, in *The Genetics and Biology of* Drosophila, M. Ashburner and T. Wright, Eds. (Academic Press, London, 1980), vol. 2d, p. 141.
15. D. Montell, P. Rorth, A. Spradling, *Cell* **71**, 51 (1992).
16. Germline clones were generated by irradiating with x-rays larvae of the genotype *ru spn-C*^{094} *st e ca/ P[ovo*^{D1}*]*^{2x48}, essentially as described [T.-B. Chou, E. Noll, N. Perrimon, *Development* **119**, 1359 (1993)]. We dissected 2500 females to find 11 visible clones in the ovaries. About 30% of the chimeric egg chambers showed the *spn-C* phenotype.
17. S. Goode, D. Wright, A. P. Mahowald, *Development* **116**, 177 (1992).
18. D. St Johnston, D. Beuchle, C. Nüsslein-Volhard, *Cell* **66**, 51 (1991).
19. E. Giniger, W. Wells, L. Jan, Y. Jan, *Roux's Arch. Dev. Biol.* **202**, 112 (1993).
20. H.-K. Cheung, T. Serano, R. Cohen, *Development* **114**, 653 (1992).
21. F. Neuman-Silberberg and T. Schüpbach, *Cell* **75**, 165 (1993).
22. M. Peifer, S. Orsulic, D. Sweeton, E. Wieschaus, *Development* **118**, 1191 (1993).
23. Mutations in the *spn-A, spn-B,* and *spn-D* genes (*10*) result in a very similar phenotype to *spn-C*, and in all cases the misplacement of the oocyte has the same consequences on the establishment of AP polarity in the egg chamber, as determined by the *slbo* expression in the follicle cells and the localization of osk and bcd mRNAs within the oocyte (*25*).
24. R. Chasan and K. Anderson, in (*13*), pp. 387–424.
25. A. González-Reyes and D. St Johnston, unpublished data.
26. Actin filaments were stained with rhodamine-labeled phalloidin as described [F. Xue and L. Cooley, *Cell* **72**, 681 (1993)]. The images from different focal planes were collected with the use of confocal microscopy.
27. For Hoechst staining, fixed ovaries were incubated 3 min with Hoechst (10 mg/ml, Sigma) and mounted in 70% glycerol. X-gal staining was as described (*15*).
28. The in situ hybridizations were performed as described [P. Ingham, *Nature* **366**, 560 (1993)] and immunohistochemistry as described (*18*). We used the transgenic line KZ32 as a source of kinesin–β-galactosidase protein (*6*).

29. We wish to thank I. Clark, R. Cohen, T.-B. Chou, D. Montell, F. Neuman-Silberberg, N. Perrimon, T. Serano, and T. Schüpbach for supplying us with fly strains and plasmids and for sharing unpublished results; O. Dunin-Borkowski for advice on protocols; N. Brown, J. Casanova, and M. D. Martín-Bermudo for comments on the manuscript; and M. Weston for Fig. 3E. We are also grateful to our colleagues in the lab for their helpful discussions and advice. A.G.-R. is a European Molecular Biology Organization postdoctoral fellow. This work was supported by a Wellcome Trust Senior Fellowship to D.StJ.

21 June 1994; accepted 25 August 1994

An AIDS-Like Condition Induced in Baboons by HIV-2

Susan W. Barnett, Krishna K. Murthy, Brian G. Herndier, Jay A. Levy*

Six baboons (*Papio cynocephalus*) were intravenously inoculated with the human immunodeficiency virus–type 2 (HIV-2) strain HIV-2_{UC2}. All seroconverted within 6 weeks after inoculation; five animals became persistently infected. Four developed lymphadenopathy, and three of the animals had $CD4^+$ T cell loss within 18 to 24 months after inoculation. One of these baboons, showing severe clinical symptoms, showed at necropsy widespread dissemination of virus with follicular depletion in the lymph nodes, extensive fibromatosis involving lymphoid and nonlymphoid tissues, and lymphocytic interstitial pneumonitis. Another animal is cachectic and exhibited lymphoid follicular lysis and fibrous skin lesions. Other baboons inoculated with a second strain, HIV-2_{UC14}, have shown evidence of persistent infection. HIV-2 infection of baboons provides a valuable animal model for studying HIV persistence and pathogenesis and for evaluating approaches to antiviral therapies.

Despite advances in our understanding of acquired immunodeficiency syndrome (AIDS) and its etiologic agents HIV-1 and HIV-2, there is no well-established animal model to study potential therapies and vaccines for HIV-induced diseases. Of the nonhuman primates, the chimpanzee (*1*) and the pig-tailed macaque *Macaca nemestrina* (*2*) are the major species susceptible to HIV-1 infection. Apart from some symptoms of acute infection observed in the macaque model, in neither of these systems have animals developed signs of disease. In the case of the chimpanzee, this fact, together with their endangered species status and cost (*3*), makes their clinical use problematic. Moreover, most evidence indicates that reproducible persistent infection of *M. nemestrina* with HIV-1 strains cannot be achieved (*4*).

Although HIV-2 infection was previously reported mostly in West African countries, there is now evidence of its presence in other parts of the world, par-

S. W. Barnett and J. A. Levy, Department of Medicine and Cancer Research Institute, School of Medicine, University of California, San Francisco, CA 94143, USA.
K. K. Murthy, Southwest Foundation for Biomedical Research, San Antonio, TX 78228, USA.
B. G. Herndier, Department of Pathology, School of Medicine, University of California, San Francisco General Hospital, San Francisco, CA 94110, USA.

*To whom correspondence should be addressed.